Deviation from the Fano profile in resonance-enhanced multiphoton autoionization

Lipika Adhya and Krishna Rai Dastidar

Atomic and Molecular Physics Section, Department of Materials Science, Indian Association for the Cultivation of Science, Jadavpur, Calcutta 700032, India (Received 28 February 1994)

We know that the Fano profile is obtained for single-photon absorption to the ionization continuum in the presence of an autoionizing state. We have shown that, in the case of (1+1)-photon absorption to an autoionizing state embedded in the ionization continuum, the absorption profile changes radically to a mirror image of the Fano profile for the value of $q = \pm 1$, q being the Fano q parameter. Moreover, for higher values of q, the (1+1)-photon absorption profile exhibits a broad minimum, while a distinct interference pattern is obtained in the profile of single-photon absorption. The absorption line shape has been found to oscillate between the Fano and a modified Fano profile for the autoionization through odd and even number of steps, respectively, via resonances.

PACS number(s): 32.80.Rm, 32.80.Dz

It is well known that in case of single-photon excitation to an autoionizing (AI) state embedded into the ionization continuum, the direct ionization channel interferes with the autoionization channel leading to an asymmetric Fano-type profile for the absorption line shape [1]. Similarly, a Fano profile can also be obtained for m-photon nonresonant transitions where the single-photon dipoletransition moments have to be substituted by m-photon terms. The purpose of this work is to show that in the case of resonance-enhanced multiphoton ionization or autoionization [i.e., (m+n)-photon REMPAI], this interference pattern and also the q dependence of the absorption profile change radically from the Fano character. To demonstrate this, we have considered here single-photon and (1+1)-photon autoionization and ionization. Moreover, by considering (1+1+1)-photon and (1+1+1+1)-photon transitions, we have shown that Fano and modified-Fano profiles occur alternately for absorption through odd and even numbers of steps, respectively, via resonances.

A few different transition schemes are shown below:

(i) Single-photon:

$$\begin{array}{ccc} |g\rangle|n\rangle & \stackrel{\hbar\omega}{\rightarrow} & |a\rangle|n-1\rangle \\ & \downarrow & V_{ac}(\text{configuration interaction}) \\ & |c\rangle|n-1\rangle & \end{array}$$

(ii) (1+1)-photon:

$$\begin{array}{ccc} |g\>\rangle|n\>\rangle & \stackrel{\hbar\omega}{\to} |i\>\rangle|n-1\>\rangle \stackrel{\hbar\omega}{\to} & |a\>\rangle|n-2\>\rangle \\ & \downarrow & V_{ac} \\ & |c\>\rangle|n-2\>\rangle \end{array} \label{eq:polyanting}$$

(iii) (1+1+1)-photon:

$$\begin{array}{ccc} |g\>\rangle|n\>\rangle\stackrel{\hbar\omega}{\to}|i\>\rangle|n-1\>\rangle\stackrel{\hbar\omega}{\to}|m\>\rangle|n-2\>\rangle\stackrel{\hbar\omega}{\to}|a\>\rangle|n-3\>\rangle\\ &\downarrow &V_{ac}\>.\\ |c\>\rangle|n-3\>\rangle \end{array}$$

The (1+1+1+1)-photon transition has a similar scheme,

except with an additional intermediate resonant state $|s\rangle$ (Fig. 1). Here $|g\rangle|n\rangle, |i\rangle|n-1\rangle, |a\rangle|n-2\rangle$; etc., are the product states: $|g\rangle, |i\rangle, |c\rangle$, are the atomic or molecular states and the $|n\rangle$'s are the photon number states.

Starting from the resolvent operator [2-4] equation,

$$(Z-H)G(Z)=1, (1)$$

a set of equations for the matrix elements of the resolvent operator is derived by projecting out the product states as follows; for single-photon autoionization,

$$(Z - E_g)G_{gg} - D_{ga}G_{ag} - \int D_{gc}G_{cg}dE_c = 1$$
, (2a)

$$(Z - E_a)G_{ag} - D_{ag}G_{gg} - \int V_{ac}G_{cg}dE_c = 0$$
, (2b)

$$(Z - E_c)G_{cg} - D_{cg}G_{gg} - V_{ca}G_{ag} = 0$$
, (2c)

and for (1+1)-photon autoionization via the intermediate resonant state $|i\rangle$,

$$(Z - E_g)G_{gg} - D_{gi}G_{ig} = 1$$
, (3a)

$$(Z - E_i)G_{ig} - D_{ig}G_{gg} - \int D_{ic}G_{cg}dE_c - D_{ia}G_{ag} = 0$$
, (3b)

$$(Z - E_a)G_{ag} - D_{ai}G_{ig} - \int V_{ac}G_{cg}dE_c = 0$$
, (3c)

$$(Z - E_c)G_{cg} - D_{ci}G_{ig} - V_{ca}G_{ag} = 0$$
, (3d)

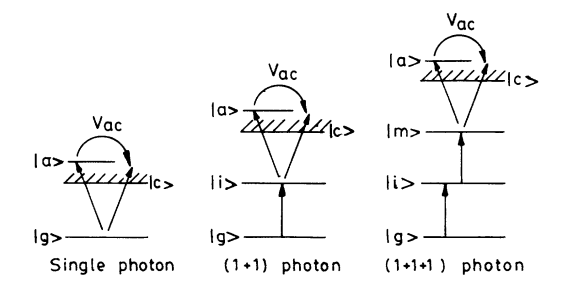


FIG. 1. Schematic diagram of the single-photon and resonant multiphoton transitions.

50

where E_g , E_i , E_a , E_c , are the energies for the product states; the D_{pq} 's are the dipole-transition moments, coupling product states $|p\rangle$ and $|q\rangle$; and V_{ca} is the configuration interaction between the continuum and the Al state $|a\rangle$. In both cases, a formal expression for G_{cg} can be obtained from Eqs. (2c) and (3d), respectively. Substituting this in other equations, one can obtain a set of two equations for the single photon and a set of three equations for (1+1)-photon autoionization, respectively. The above method can be extended to obtain corresponding equations for (1+1+1)-photon autoionization.

By solving these equations, the matrix elements for resolvent operators can be written as

$$G_{pq}(Z) = \frac{f_p(Z)}{Z - Z_0}$$
, (4)

in the weak-field limit. Since Z_0 is the pole of the resolvent operator, it gives the complex energy of the total system (atom or molecule plus photon) and the imaginary part of Z_0 is proportional to the decay rate of the system. The matrix elements of evolution operator $U_{pq}(t)$ can be obtained as an inverse Laplace transform of $G_{pq}(Z)$ and hence $|U_{pq}(t)|^2$ gives the population at time t in the respective state $|p\rangle$. Therefore, in the weak-field limit the probability of ionization is given as $P(t) = 1 - |U_{gg}(t)|^2$ and hence the rate of ionization can be obtained in the limit $t \to 0$ as

$$\frac{dp}{dt} = -2 \operatorname{Im} Z_0 , \qquad (5)$$

where the Z_0 's at Z=0 are given as the following.

(i) For single-photon transition,

$$Z_{01} = \frac{\gamma_g}{2} \frac{i(\varepsilon + i) - (q - i)^2}{(\varepsilon + i)}.$$

(ii) For (1+1)-photon transition,

$$Z_{02} = \frac{|D_{gi}|^2}{\gamma_i/2} \frac{(\varepsilon + i)}{i(\varepsilon + i) - (q - i)^2}$$
.

The γ_j 's are the photoionization widths for the states $|j\rangle$, ε is detuning (δ) from the AI states in units of autoionization half-width ($\Gamma/2$), and q is the Fano-q parameter,

$$q = \frac{D_{ja} + P \int \frac{D_{jc} V_{ca}}{E - E_c} dE_c}{\pi D_{jc} V_{ca}|_{E_c = E}} ,$$

where $|j\rangle$ corresponds to the final resonant state from which ionization occurs.

Hence the decay rates are given as follows.

(i) Single-photon:

$$\frac{dp_1}{dt} = A_1 F_1(q) ,$$

where

$$A_1 = \frac{\gamma_g}{2}, \quad F_1(q) = \frac{(\varepsilon + q)^2}{(1 + \varepsilon^2)}$$
.

(ii) (1+1)-photon:

$$\frac{dp_2}{dt} = A_2 F_2(q) ,$$

where

$$A_2 = \frac{|D_{gi}|^2}{\gamma_i/2}, \quad F_2(q) = \frac{(\varepsilon + q)^2}{q^4 + (\varepsilon + 2q)^2}$$
.

It can easily be shown that for (1+1+1)-photon and (1+1+1+1)-photon autoionization or ionization, the decay rates are

$$\frac{dp_3}{dt} = A_3 F_3(q), \quad \frac{dp_4}{dt} = A_4 F_4(q),$$

where

$$A_3 = \frac{\gamma_m}{2} \frac{|D_{gi}|^2}{|D_{im}|^2}, \quad A_4 = \frac{|D_{gi}|^2}{|D_{im}|^2} \frac{|D_{ms}|^2}{\gamma_s/2},$$

and where

$$F_3(q) = F_1(q), F_4(q) = F_2(q)$$
.

Here, $F_1(q)$ and $F_2(q)$, when plotted as a function of ε , give rise to the Fano and modified Fano profiles, respectively. Since $F_3(q) = F_1(q)$ and $F_4(q) = F_2(q)$, it is obvious that the Fano and modified Fano profiles will also be obtained for (1+1+1)-photon and (1+1+1+1)-photon resonant absorption. Therefore, the Fano and modified Fano profiles will be obtained alternately for transitions through odd and even numbers of steps, respectively.

We will now show that the phase of the complex energy will also shuttle back and forth between two values $\pi + \alpha$ and $2\pi - \alpha$ in the above cases. The complex energy Z_0 's can be written as

$$Z_{0n} = r_n e^{i\theta} n$$
,

where r_n and θ_n are the modulus and phase of Z_0 's in the complex energy plane. By rationalizing Z_0 's, one can obtain

$$Z_{01} = A_1 \frac{-C - iD}{(\varepsilon^2 + 1)}, \quad Z_{02} = A_2 \frac{C - iD}{a^4 + (\varepsilon + 2a)^2},$$

where $C = \varepsilon(1-q^2) + 2q$ and $D = (\varepsilon + q)^2$. Hence

$$\tan\theta_1 = \frac{-D}{-C}$$
, $\tan\theta_2 = \frac{-D}{C}$.

Here D is always positive. C can be either positive or negative. When C is positive, Z_{01} will be in the third quadrant and Z_{02} will be in the fourth quadrant of the complex energy plane (Fig. 2). Similarly, for C negative, the situation is reversed. Therefore, the θ 's can be related as

$$\theta_n = \theta_{n-1} + (-1)^n (\pi - 2\alpha)$$

where $\theta_1, \theta_2, \theta_3$ can be derived as $\theta_1 = \pi + \alpha$, $\theta_2 = 2\pi - \alpha$, $\theta_3 = \pi + \alpha$, and so on. Hence $\sin \theta_1 = \sin \theta_2 = -\sin \alpha$. The

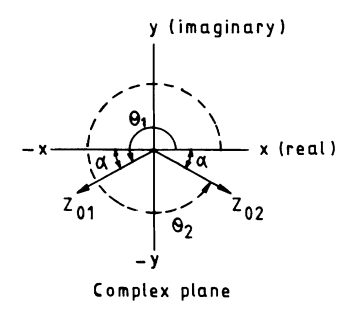


FIG. 2. The position of the poles of the resolvent operator for single-photon and (1+1)-photon autoionization in the complex energy plane.

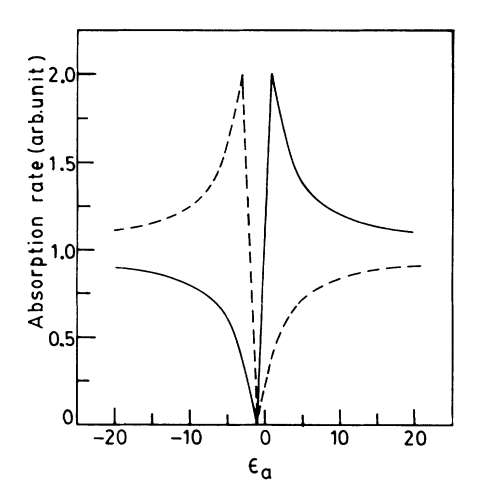


FIG. 3. —, absorption profile for single-photon AI. --, absorption profile for (1+1)-photon AI. $D_{ig}=0.5$, q=1.0.

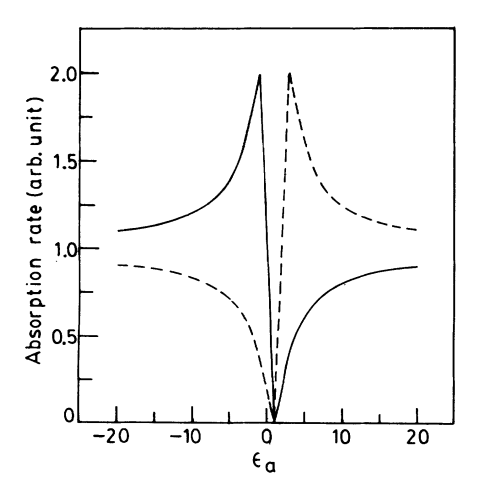


FIG. 4. Same as Fig. 3, except q = -1.0.

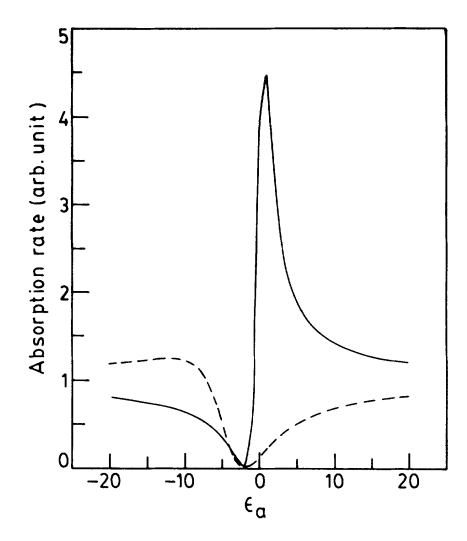


FIG. 5. Same as Fig. 3, except q=2.0.

modulus r_n 's can be written as

$$r_n = \frac{dp_n}{dt} \frac{1}{2\sin\theta_n} .$$

Therefore, with the addition of subsequent resonant steps in the ionization or autoionization process, the Z_0 's in the complex energy plane are given by the general expressions $r_n \exp(i\theta_1)$ and $r_{n+1} \exp(i\theta_2)$ (where $n=1,3,5,\ldots$) for odd and even numbers of resonance steps, respectively. In the former case the absorption is given by the Fano profile, while in the latter case the modified profile $F_2(q)$ is obtained.

Figures 3-6 show the absorption profiles for single-photon and (1+1)-photon autoionization as a function of ϵ for different values of q. Figures 3 and 4 show the autoionization line shape for single-photon and (1+1)-photon transition schemes for q=+1 and -1, respectively. It is found that the profile for (1+1)-photon transition looks somewhat like the mirror image of that for the single-photon transition about a vertical plane through $\epsilon=-q$. With the increase in value of q (Fig. 5),

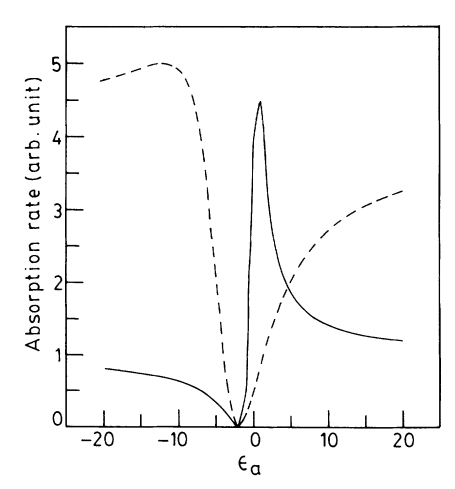


FIG. 6. Same as Fig. 5, except $D_{ig} = 1.0$.

the single-photon Fano profile shows sharp interference whereas the (1+1)-photon autoionization or ionization profile shows a damped and broadened profile, i.e., minimum and maximum spread over a larger range of ϵ . This damping is governed by the relative strength of the first step transition. If the transition strength of the first step excitation is increased (Fig. 6), the (1+1)-photon autoionization or ionization profile shows a stronger interference effect despite being broadened.

In conclusion, we have shown that for autoionization

or ionization through an even number of steps (via resonances), the autoionization profile deviates radically from the Fano shape. This modified profile exhibits a minimum in a wide range of frequencies for large values of q (unlike the Fano profile), which may be utilized in order to minimize the loss in the laser system.

This work has been sponsored and supported by the Department of Science & Technology, New Delhi, under Project No. SP/S2/L-20/90.

(1992)

^[1] U. Fano, Phys. Rev. A 124, 1866 (1961).

^[2] K. Rai Dastidar and P. Lambropoulos, Phys. Rev. A 29, 183 (1984).

^[3] L. Adhya and K. Rai Dastidar, Nuovo Cimento D 14, 643

^[4] S. Sanyal, L. Adhya, and K. Rai Dastidar, Phys. Rev. A 49, 5135 (1994).